J Indian Inst Sci, May–June 1992, **72**, 235–260.

Dispersion in stirred vessels

R. KUMAR
Department of Chemical Engineering, Indian Institute of Science AND Jawaharlal Nehru Centre for Advanced Scientific Research, Bangalore 560 012, India

Abstract

The three-dimensional problem of drop breakage in stirred vessels can be successfully reduced to a single-dimensional framework using Voigt element, retaining the essential features of the breakage process Recent models successfully employ it to predict the maximum stable drop diameter, d_{max}, for not only rheologically complex dispersed phases, but also when surfactants or drag-reducing agents are present in the continuous phase

The effect of the dispersed phase hold up on d_{max} shows trends contrary to expectation This can be explained only by invoking two new mechanisms of drop breakage, each giving its own d_{max} The observed d_{max} therefore is the minimum of the three d_{max} values given by the three mechanisms.

A multistaged model, developed recently, explains the reducing influence of the dispersed phase viscosity, μ_d, at high μ_d values It also explains how the interfacial tension continues to influence d_{max} under these extreme conditions.

A new model for breakage frequency based on unequal breakage and eddy size distribution existing in the vessel is able to predict not only the breakage frequency, but also the daughter droplet size distribution.

Key words: Drop breakage, maximum stable drop diameter, breakage frequency, stirred vessel.

1. Introduction

Stirred vessels find extensive use in chemical industry, particularly in the manufacture of high-value, low-volume fine chemicals. They permit continuous or batch operation and can handle single or multiple phases. Though extensively employed, the quantitative understanding of their performance is at a rudimentary stage even for the simple case of their handling homogeneous reactions. The normal assumption made while analysing single phases is that the mixing in the vessel is instantaneous and hence the parameters of interest like temperature and concentration of the species are uniform in the vessel. This approach is quite satisfactory while analysing slow chemical reactions. However, as the reactions become very fast, this approach fails and large deviations from its predictions are observed experimentally. Bourne *et al*[1], while trying to demonstrate segregation in stirred vessels, used the following scheme of reactions:

$$A + B \rightarrow R \text{ (fast reaction)}$$

$$R + B \rightarrow S \text{ (slow reaction)}$$

where A is 1-napthol, B sulphanilic acid, R, 4-(4′-sulphophenyl azo)-1-napthol (monoazodye), and S, 2,4-bis(4′-sulphophenyl azo)-1-naphthol (bis azo dye).

The reaction velocity constant for reaction between A and B is 150 times higher than that between R and B. As B is added to A and it mixes instantaneously, most of the B will immediately react to form R and hence the amount of S formed would be very small. This could be calculated in a straightforward way through the well-mixed idealisation. However, a comparison between the observed concentrations of S with the calculated values showed that the observed concentrations were orders of magnitude higher than the calculated ones. When B is added to stirred vessel, already containing A, the turbulence in the vessel breaks the lumps of B into smaller and smaller lumps, and eventually B has to diffuse and react with A in the bulk. The breakage of B into tiny fragments increases enormously the area available for diffusion, but the final mixing occurs through molecular diffusion. It is only when the characteristic time for diffusion is much lower than the characteristic time for reaction, the well-mixed assumption can hold good. For fast reactions, the two become either of the same order of magnitude or the characteristic reaction time becomes much lower than the diffusion time. Under this condition the vessel contents have to be assumed to be segregated and an analysis based on diffusion-reaction concept has to be employed. A number of such models[2-4] are available in literature which try to incorporate these concepts, and simultaneously bring out the complex nature of the stirred vessel even for apparently simple homogeneous systems.

When another immiscible phase is introduced in a stirred vessel already containing a liquid, as in the case of a mixer-settler, the situation becomes much more complex. The new phase has to break up and form the dispersed-phase droplets, which provide the interfacial area across which the mass and heat transfer occur. Further, the drops continuously coalesce with each other and break again. The mixing of the dispersed phase is entirely decided by the processes of coalescence and re-dispersion, even though the continuous phase could be assumed to be well mixed. It is necessary to be able to predict the drop sizes as well as the coalescence and breakage phenomena to be able to quantitatively explain the performance of such a stirred vessel contactor. There are two approaches available to make such predictions. The conventional approach assumes that all the drops in the vessel are identical in size, temperature and concentration and each has the same transfer coefficient. Thus, the processes of breakage and coalescence are lumped together in defining average quantities. The average drop diameter, called the 'Sauter mean diameter', is defined in a fashion that the total interfacial area in the vessel is conserved. The area per unit volume of the dispersion is related to the 'Sauter mean diameter', d_{32}, by the expression:

$$a = \frac{6\phi}{d_{32}} \cdot \tag{1}$$

The d_{32} can be calculated rigorously, only if the complete drop-size distribution is

known, which in turn involves the detailed knowledge of the breakage and coalescence rates. It has no simple theoretical basis. However, a large body of experimental data shows that the largest stable drop diameter, d_{max}, is 1·5 to 1·6 times the value of d_{32}. As d_{max} has a simple theoretical basis, attempts have been made by many investigators to develop models for predicting d_{max} and then obtaining d_{32} from it by using the empirical factor obtained from experiments. Though successful, in many situations, the use of d_{32} can lead to serious deviations from reality. Schumpe and Deckwer[5] have shown that averaging can lead to predictions which differ significantly from experimental observations. Under these conditions it is necessary to predict the drop size distribution by taking the coalescence and breakage phenomena into account through the framework of population balance equations[6]. These equations make a number balance for particles of size between v and $v + dv$, by considering that these numbers can change through various birth and death processes. For a stirred vessel, the number balance equation is:

$$\frac{\partial n(v,\ t)}{\partial t} = \underbrace{\int_v^\infty \Gamma(v')\ n(v',t)\ \beta(v,\ v')\ \gamma(v')\ dv'}_{\text{I}} - \underbrace{\Gamma(v)\ n(v,\ t)}_{\text{II}}$$

$$+ \underbrace{\int_0^{v/2} q(v - v',\ v')\ n(v - v',\ t)\ n(v',\ t)\ dv'}_{\text{III}}$$

$$- \underbrace{\int_0^\infty q(v,\ v')\ n(v,\ t)\ n(v',\ t)\ dv'}_{\text{IV}} + \underbrace{N_0(v,\ t)}_{\text{V}} - \underbrace{n(v,\ t)\ f_0(v)}_{\text{VI}} \cdot \tag{2}$$

The above equation is in terms of number density, but when multiplied by dv, each term corresponds to the actual number of drops of size between v and $v + dv$, being formed or removed. Term I corresponds to the rate of formation of these drops by breakage of larger drops whereas the second term gives the death rate of these drops due to breakage. Term III represents the formation due to coalescence of drops of size $(v - v')$ with those of size v' whereas Term IV stands for their removal due to their coalescence with the other drops. Terms V and VI signify the input and escape rates, respectively. For batch-stirred vessels, these two terms vanish. Equation (2) cannot be solved as it stands. It is necessary to have expressions for the breakage frequency, $\Gamma(v)$, the daughter droplet distribution, $\beta(v,\ v')$, when a drop breaks, the number of drops formed $\gamma(v')$ when a drop of size v' breaks and the coalescence frequency. These expressions need to be incorporated in eqn (2) before it can be solved. Even for predicting $\Gamma(v)$ and $\beta(v,\ v')$, it is necessary to be able to predict d_{max}, as that is the size at which breakage frequency would become zero and it would not yield any daughter droplets. Though coalescence is important, the present work is concerned mainly with breakage both for prediction of d_{max} and for developing expressions for breakage frequency and daughter-droplet distribution.

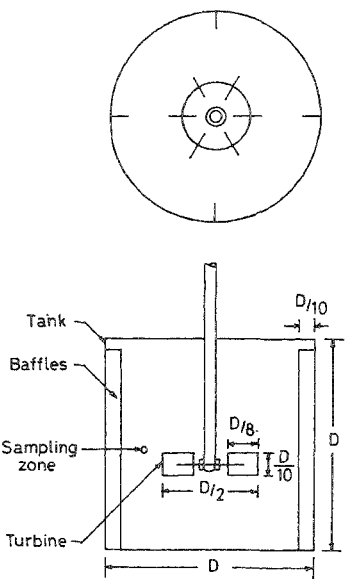

FIG. 1 A stirred vessel with Rushton impeller.

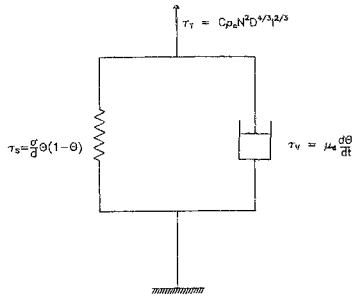

FIG. 2. Voigt element representation of drop breakage.

2. Measurement and prediction of the maximum stable drop diameter, d_{max}

2.1. *Measurement of* d_{max}

A typical stirred vessel with a Rushton impeller is shown in Fig. 1. Though the mechanism of drop breakage will not change with the nature of impeller, the numerical values of the constants associated with turbulence will vary. Hence the work discussed in the present paper is directly applicable to Rushton impellers whereas the concepts are applicable to other impellers also. In order to experimentally determine the d_{max} value, the continuous phase is taken in the stirred vessel and the stirrer speed adjusted to the desired rps value. The dispersed phase in the desired volume fraction is then added and the stirrer permitted to run at the desired speed. Samples of dispersed phase drops are scanned from the zone just outside the impeller and d_{max} value is obtained. When d_{max} does not change as a function of time, that value is taken to be the correct d_{max} value. To be sure of the measurement, many investigators measure d_{32} values from the same region simultaneously and check if the ratio of d_{max} to d_{32} falls in the empirically obtained ratio of 1·5 to 1·6. For dispersed

phases of high viscosity, this ratio is known not to hold. However, the simultaneous measurement of both d_{max} and d_{32} does help in ensuring that d_{max} is in the right range.

2.2. *Prediction of d_{max} for inviscid dispersed phases*

The existence of d_{max} is based on the concept that drops deform and break due to the action of turbulence velocity fluctuations across them which are also referred to as drop-eddy interactions. When a drop is interacted by a much larger eddy, it is simply convected without resulting in breakage. When, however, an eddy of the same size as the drop diameter interacts with it (pressure fluctuation across the diameter of the drop), it imposes an inertial stress on the drop causing a deformation. As the drops deform, the interfacial stress, also called elastic stress, comes into play which tends to restore the drop to its original shape. The inertial stress increases as the drop size increases, whereas the interfacial tension stress increases as the drop size decreases. Thus, for a very large drop, the inertial stress is very high whereas the interfacial tension stress is low This results in drop breakage. As the drop becomes smaller, the inertial stress decreases whereas the interfacial tension stress increases. Thus, a drop size is finally reached, where the inertial stress is just unable to fragment the drop, giving rise to the largest possible drop which is stable. The actual drop has a flow field around it and this three-dimensional flow causes both the flow inside the drop and its deformation. However, at the present stage of understanding of the phenomenon, it is not possible to analytically analyse this complex situation in detail and predict the sizes of the fragments. Instead, first-generation models are developed which capture the gross features of breakage phenomenon but bypass the detailed flow fields both outside and inside the drop. Kolmogorov[7] and Hinze[8] were the earliest investigators to employ this concept for the prediction of d_{max}. They considered that for a drop to break, the critical ratio between the kinetic energy of the eddy, $\rho_c \overline{u^2(d)} d^3$, and the surface energy of the drop σd^2, must exceed a critical value. Data on turbulence characteristics in a stirred vessel using Rushton impeller show that approximately 60% of the energy imparted by the impeller to the liquid is dissipated in the vicinity of the impeller. The volume of this region is only about 10% of the total volume of the total liquid. Thus, the region near the impeller where the breakage phenomenon is predominant is a zone of high-turbulence intensity. Data further show that the energy spectra here show a $-5/3$ slope in the higher frequency range, leading to the conclusion that the turbulence can be considered homogeneous and isotropic. This facilitates the application of the energy cascade theory to estimate the energy contained in the eddies in the inertial range, which is of relevance to drop breakage. Under these conditions the mean square velocity fluctuations can be expressed as:

$$\overline{u^2(d)} \propto \epsilon^{2/3} d^{2/3}. \tag{3}$$

For stirred vessels, ϵ can be expressed in terms of stirrer and operating parameters as:

$$\epsilon \propto N^3 D^2. \tag{4}$$

Substitution of eqns (3) and (4) in Hinze's criterion leads to:

$$\frac{d_{max}}{D} = \text{constant } We^{-0.6} . \tag{5}$$

Sprow[9] has found the constant to vary between 0·126 and 0·15, whereas Lagisetty *et al*[10] found it to be 0·125. A number of investigators have employed eqn (5) or some variation of it to explain their data. Coulaloglou and Tavlarides[11] have discussed most of the correlations, based on eqn (5) available in literature.

2.3. *Prediction of d_{max} for viscous and non-Newtonian dispersed phases*

Equation (5) can be employed when the viscosity of the dispersed phase is very low, as it does not involve any term containing the dispersed-phase viscosity. Experimentally, however, the dispersed-phase viscosity has been found to have significant effect on d_{max}[10,12–15]. All these authors find that d_{max} increases with increase in dispersed-phase viscosity. When a viscous drop is acted upon by an eddy, its deformation is retarded not only by the shape-restoring interfacial stress but also by the flow-retarding viscous stress. In the single-dimension framework, Arai *et al*[12] tried to account for these by considering the breakage process to be represented by a Voigt element. Because of a series of assumptions made by them regarding the nature of the spring and the periodic nature of turbulent fluctuations, they could not explain their data with the model and used a semi-empirical expression. The model does not yield the low-viscosity limit and cannot be employed for rheologically more complex fluids.

Lagisetty *et al*[10], while pointing out the various deficiencies in the model of Arai *et al*[12], considered the basic framework provided by Voigt element to be reasonable. They, therefore, developed a model based on it. The Voigt element consisting of a spring and dashpot assembly is shown in Fig. 2. Unlike the earlier model, they considered that the breakage would occur within the life time of an eddy, during which the inertial stress on the drops remains uniform. They further assumed that the interfacial tension stress passes through a maximum. This assumption was based on the findings of Rallison[16] who reported that near the breakage point the interfacial tension aids rather than retarding the drop breakage. Thus, they assumed a nonlinear spring $\frac{\sigma}{d}\theta(1-\theta)$ as one component of the Voigt element. This clearly gave a physical description of the breakage process, as a drop having a deformation of unity would not be able to retract and hence could be considered broken. They took a general rheological expression $\left(\tau_0 + K\left(\frac{d\theta}{dt}\right)^n\right)$ for the dashpot. It is seen from Fig. 2 that the applied turbulent stress τ_t must be equal to the sum of the two resisting stresses. Further, in a Voigt element, the deformation of the spring and the dashpot at any time are equal. Thus,

$$\tau_t = \frac{\sigma}{d}\theta(1-\theta) + \tau_0 + K\left(\frac{d\theta}{dt}\right)^n . \tag{6}$$

τ_t is proportional to $\rho_c \overline{u^2(d)}$. Use of eqns (3) and (4) in this expression yields

$$\tau_t = C\ \rho_c N^2\ D^{4/3}\ d^{2/3}\ . \tag{7}$$

Thus,

$$C\ \rho_c\ N^2\ D^{4/3}\ d^{2/3} - \tau_0 = \frac{\sigma}{d}\,\theta(1-\theta) + K\left(\frac{d\theta}{dt}\right)^n. \tag{8}$$

Equation (8) describes the deformation dynamics of the drop and can be solved with the initial condition of zero deformation. The value of d_{max} is then computed so that the time required for deformation to reach unity is equal to the life time of the eddy. Equation (8) can be expressed in the dimensionless form:

$$C\ We\left(\frac{d}{D}\right)^{5/3} - (\theta - \theta^2) - \left(\frac{\tau_0 d}{\sigma}\right) = \left(\frac{d\theta}{d\eta}\right)^n \tag{9}$$

where η is the dimensionless time given by $t/\left(K\dfrac{d}{\sigma}\right)^{1/n}$. The initial condition in dimensionless form becomes:

$$\theta = 0 \text{ at } \eta = 0.$$

From the solution of eqn (9), η required to reach $\theta = 1$ is computed, and compared with the dimensionless life time of the eddy. d_{max} is obtained when

$$\eta(\theta = 1) = \frac{\bar{T}}{\left(\dfrac{Kd_{max}}{\sigma}\right)^{1/n}}\ . \tag{10}$$

The expression for $\bar{T}$ is

$$\bar{T} = \frac{1}{N}\left(\frac{d}{D}\right)^{2/3}\ . \tag{11}$$

Equation (9) has been solved by Lagisetty *et al*[10] for various values of n. The value of C found by them from their experimental data works out to be 8 giving the proportionality constant of 0·125 which is quite close to the value reported by Sprow[9]. No extra coefficient is employed in their model while taking the rheology of the drop phase into account. The solution of eqn (9) obtained by them for Newtonian liquids is:

$$(Re/We)\left(\frac{d_{max}}{D}\right)^{-1/3} = [1/(4\alpha - 1)^{1/2}]\ \tan^{-1}\ [1/(4\alpha - 1)^{1/2}] \tag{12}$$

where α is equal to $8We(d_{max}/D)^{5/3}$. The model correctly yields eqn (5) as the limiting case for inviscid dispersed phases.

Lagisetty *et al*[10] have tested this model for Newtonian liquids of different viscosities, Bingham plastics as well as dispersed phases following power law rheology and found it to be satisfactory. Figure 3 presents a comparison of their model for Newtonian liquids, with the data of Arai *et al*[12]. The points in the figure are experimental whereas the lines are based on the model. The agreement in this range of viscosities is excellent.

The basic framework has been successfully extended to predict d_{max} values when the dispersed phase is mildly viscoelastic[17], or when surfactants[18] or drag-reducing agents[19] are present in the continuous phase. However, the model could not predict the behaviour of highly viscoelastic dispersed phases which tend to form globules and strands rotating around the impeller without breakage.

The condition of breakage ($\theta = 1$, during the life time of the eddy) is somewhat arbitrary. The shear flow assumed inside the drop during deformation is also open to criticism. Gandhi and Kumar[20] have developed an elongational flow framework in which the drop elongates into a cylindrical jet on the application of the turbulent stress. They applied the breakage condition based on the jet-stability analysis. The maximum stable drop sizes predicted by them are the same as those predicted by the model of Lagisetty *et al*[10]. Hence, at present, it is not possible to comment conclusively on the relative merits of the two models, even though the elongational flow model uses more realistic condition for drop breakage.

3. Alternative mechanisms of drop breakage

One of the tacit assumptions made in the development of the models discussed above is that the presence of dispersed phase does not influence the turbulence characteristics existing in the vessel. Hence, the dispersed-phase hold up in the vessel does not appear in the expressions described above. To keep the influence of the presence of the dispersed phase on the turbulence characteristics in the vessel as small as possible, most of the breakage experiments reported in literature employed very low hold-up ($< 0{\cdot}05$) values. However, such investigations, though highly useful from the point of view of understanding the phenomenon, cannot be directly employed in industry where high hold-up values are employed.

Thus attempts have been made by various investigators to predict d_{max} as a function of the dispersed-phase hold up, ϕ. It has been experimentally observed that d_{max} increases with an increase in ϕ. This is based on experiments conducted by raising ϕ up to a value of about 0·3. Empirical modifications of eqn (5) have been normally employed. The general form of the expression which has been used by many investigators[11] is:

$$d_{max}/D = C_1 (1 + C_2 \phi) We^{-0{\cdot}6} . \tag{13}$$

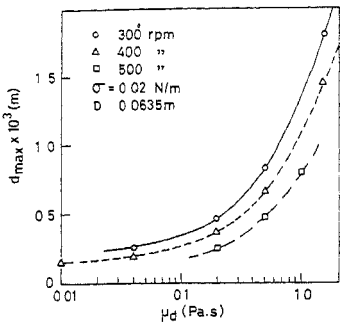

FIG 3 Comparison of the model of Lagisetty *et al*[10] with the data of Arai *et al*[12]

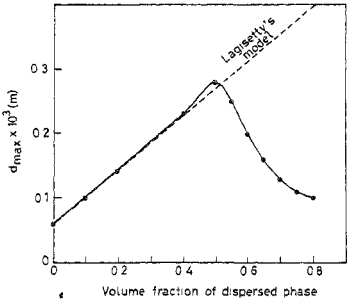

FIG. 4 Effect of ϕ on d_{max}, (—) Lagisetty *et al*[10]. Point experimental, continuous phase· water, dispersed phase· toluence, surfactant concentration: 0·3%, rps. 9·5

Lagisetty *et al*[10] incorporated the effect of ϕ by using the correlation of Lats and Frishman[21] for dampening of turbulent intensity by the presence of another phase in turbulent jets.

$$\overline{u_\phi^2(d)} = (1 + 4\phi)^{-2}\ \overline{u^2(d)}\ . \tag{14}$$

By incorporating the expression for $\overline{u_\phi^2(d)}$ into their model, they obtained the following expression for d_{max}, for inviscid dispersed phases:

$$(d_{max}/D) = 0{\cdot}125\ (1 + 4\phi)^{1{\cdot}2}\ We^{-0{\cdot}6}\ . \tag{15}$$

It is seen from this expression that d_{max} increases monotonically with ϕ. Kumar *et al*[22] conducted experiments covering a higher range of ϕ. Their results on d_{max} for toluene in water system are presented in Fig. 4. They used sodium dodecyl sulphate (0·3 wt%) in the continuous phase to suppress coalescence and make the phenomenon predominantly controlled by breakage. Along with the data points a line corresponding to the predictions made through the model of Lagisetty *et al*[10] is also drawn in the figure. It is seen that the existing model is able to explain the data up to a ϕ of about 0·4 very satisfactorily. However, at higher ϕ values, the model not only fails to predict the data, but also the qualitative trends. Beyond a ϕ of approximately 0·4, the model continues to predict increasing d_{max} values, whereas the experiments show that the d_{max} decreases with ϕ. A passing reference to the decrease of drop sizes with ϕ had also been made by Grosso *et al*[23] who did not pursue the finding further.

As this unexpected behaviour cannot be explained by the existing concepts of drop breakage through turbulent stresses, Kumar *et al*[22] proposed two hitherto unidentified

mechanisms which could also be responsible for drop breakage. These make use of the flow on the impeller itself. They proposed that the fluid accelerates along the impeller blade from its middle to the edge. At the middle of the blade it shows a stagnation point. Thus, there is a zone at the impeller where the flow is predominantly elongational. Similarly, at the impeller itself, there is a boundary layer where the flow is essentially shear. The drop could also break either under elongational or shear flow conditions, apart from the usually recognised breakage through the action of turbulent stresses. As the actual flow is highly complex, they idealised it by assuming two zones near the impeller having plane hyperbolic and plane shear flow, respectively. Drop breakage under these idealised flow conditions had already been studied by a number of investigators. As a result, they could test their hypothesis with the existing expressions available in literature.

For drop breakage in plane hyperbolic flow, they used the findings of Taylor[24] who found that the drop under this flow would break if the capillary number exceeded a critical value. Thus,

$$\frac{G_e\,(d_{max})\;\mu_e}{2\sigma} = Ca_e \cdot \tag{16}$$

The critical capillary number is a function of the viscosity ratio of the continuous and dispersed phases. As the continuous phase is an emulsion, they assumed that the drop senses the emulsion as the continuous phase and used its viscosity. The elongational strain rate G_e is not directly available. Hence, they made approximations about it by assuming the area occupied by flow to be half the area available between two adjacent blades, and flow rate being available from the expressions available for pumping rates given by a Rushton impeller. They thus obtained the following expression for G_e:

$$G_e = 50{\cdot}64\;N \cdot \tag{17}$$

Substitution of eqn (17) in (16), and rearrangement yields the expression for $(d_{max})_e$, the maximum drop size obtainable through elongational mechanism:

$$(d_{max})_e = \frac{Ca_e\sigma}{25{\cdot}32\;N\;\mu e} \cdot \tag{18}$$

They found that the residence time available in this zone is larger than the deformation time scale in their experiments by 50 to 450 times.

At the impeller blade itself, there is a boundary layer, in which they assumed simple shear flow. Here again, a critical capillary number has to be exceeded for drop breakage to occur. Thus:

$$\frac{G_s(d_{max})_s\mu_e}{2\;\sigma} = Ca_s \cdot \tag{19}$$

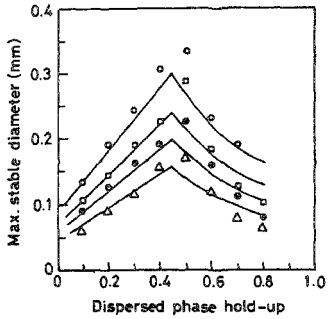

FIG. 5. Comparison of the model with experimental data: (o) 5·5 rps, (□) 6·67 rps, (●) 7·83 rps, and (△) 9·5 rps.

Evaluating G_s as (U/δ), they obtained the final expression as:

$$(d_{max})_s = \frac{Ca_s\,\sigma}{113{\cdot}2\,N^{1{\cdot}2}\mu_e^{0{\cdot}8}}\left(\frac{1}{L^2\,\rho_e}\right)^{0{\cdot}2}. \tag{20}$$

The Ca_s is a function of the ratio of the continuous and dispersed-phase viscosities. This mechanism could be operational only if the boundary-layer thickness is much higher than the drop diameter. This condition was found to be satisfied in their work.

Thus the work of Kumar *et al*[22] shows that three d_{max} values are possible in the vessel. They result from the turbulent stresses, elongational flow and shear flow. The measured d_{max} value would correspond to the minimum of these three. Actual calculations showed that at low-dispersed-phase hold-up values, the turbulent mechanism gave the lowest values. As ϕ is increased, the turbulent mechanism yields increased drop size whereas the other two mechanisms yield lowering d_{max} values. Thus, there is a crossover point, where one of the other two mechanisms yields the same d_{max} as given by the turbulent mechanism. At ϕ values higher than that, the turbulent mechanism no longer decides the d_{max} which is decided by one of the other two mechanisms. This is shown in Fig. 5 where d_{max} is plotted *versus* ϕ for various rps values. Solid lines are drawn corresponding to the minimum of the d_{max} values calculated by the three mechanisms. Up to a ϕ of about 0·4, the turbulent mechanism gave the lowest d_{max} whereas above that the shear mechanism gave the lowest values. There is a discontinuity of slope in each curve where the d_{max} values calculated by turbulent and shear mechanisms are equal.

Though the work of Kumar *et al*[22] clearly brings out the other mechanisms of drop breakage in a stirred vessel, their model is not rigorous and can be used for making

approximate calculations These approximations arise out of the drastic assumptions made both with regard to the idealisation of flow and the evaluation of the elongational strain rates and shear rates.

4. Drop breakage for highly viscous dispersed phases

The model of Lagisetty *et al*[10] discussed earlier can be used with confidence up to a dispersed-phase viscosity of approximately 1 Pa.s. Their model predicts that as viscosity is raised to very high values, the interfacial tension stress becomes negligible when compared to the viscous stress. As a result, d_{max} becomes independent of interfacial tension. Further, d_{max} would then vary as μ_d raised to the power 3/4. Calabrese *et al*[25] found that their high-viscosity data show much less dependence on μ_d than given by the 3/4th power. They empirically correlated their data by:

$$\frac{d_{max}}{D} = C \left(\frac{\mu_d}{\mu_c}\right)^{3/8} \cdot N_{Re}^{-3/4} \cdot \tag{21}$$

This correlation shows a 3/8th power dependence on the dispersed-phase viscosity. Thus, as the viscosity of the dispersed phase increases, the dependence of d_{max} on μ_d decreases from power 3/4 to lower values. Similar differences between theoretical predictions and experimental values are also observed with respect to the influence of interfacial tension. When the dispersed-phase viscosity is high, even low values of interfacial tension show strong influence on d_{max}. This is under the conditions where the model of Lagisetty *et al*[10] predicts zero influence of interfacial tension.

To quantitatively account for these differences, Kumar *et al*[26] developed a model that permits drop breakage in multiple steps. Hitherto, the whole vessel was considered as a single unit, even though it was recognised that breakage occurred near the impeller, whereas coalescence could occur in the rest of the vessel. These authors delineated the role of the two zones by considering that breakage occurs in the zone near the impellers whereas the rest of the vessel not only permits coalescence but also recirculation of the drop. They name these two zones as deformation and relaxation zones. Their idealisation of the stirred vessel is shown in Fig. 6. Unlike the earlier models, they do not assume that the breakage process has to be completed during a single eddy-drop interaction. Instead, they permit partial deformation in the zone near the impeller, under the influence of an eddy. The partially deformed drop enters the relaxation zone where the turbulent intensity is too low to add to its deformation and can hence be considered negligible. In this zone, therefore, there is no external stress acting on it and the drop tends to relax back to the original shape under the shape-restoring stress due to interfacial tension, and resisted by the viscous stress. The process of relaxation continues during the residence time of the deformed drop in this zone. If the drop does not completely retract back to its original shape, a partially deformed drop enters the deformation zone. As an initial deformation is already available, its deformation gets increased during its interaction with an eddy. Thus, an undeformed drop entering the deformation zone may require a number of

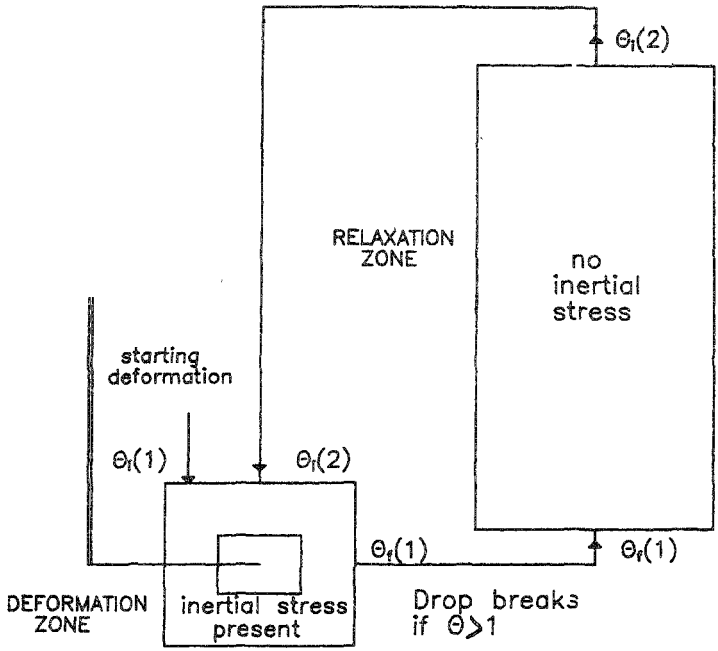

FIG. 6. Deformation and relaxation zone idealisation of the stirred vessel.

cycles for breakage. In each cycle, it may get increasingly deformed. Its final deformation in the nth cycle in the relaxation zone forms the starting condition for the deformation zone of $(n + 1)$st cycle. Alternatively, it may reach a situation where its incremental deformation in the breakage zone is exactly equal to its retraction in the relaxation zone. Then the drop would not break.

As the mechanism of deformation is the same as proposed by Lagisetty *et al*[10], the basic equation governing deformation remains the same. However, the initial condition will depend on the number of cycles. The deformation equation for the nth cycle for a Newtonian dispersed phase ($n = 1$, $K = \mu_d$) can be obtained from eqn (9):

$$\frac{d\theta_d(n)}{d\eta} = 8W_e\left(\frac{d}{D}\right)^{5/3} - (\theta_d(n) - \theta_d^2(n)) \cdot \tag{22}$$

In eqn (22), the actual value of C (= 8) of eqn (9) has been incorporated. The expression for the dimensionless life time of the eddy is:

$$\eta_d = \left(\frac{Re}{We}\right)\left(\frac{d}{D}\right)^{-1/3} \cdot \tag{23}$$

Thus, if the initial deformation for the nth cycle, $\theta_d(n)$, is specified, the final deformation, $\theta_{df}(n)$, reached at the end of the life time of the eddy, η_d, can be computed from the solution of eqn (22). For each cycle, the initial conditions of deformation are obtained at the end of relaxation zone for the previous cycle.

In the relaxation zone the equation of Lagisetty *et al*[10] is still applicable but without the turbulent stress as the turbulent intensity in this zone is very small. Under these conditions, the relaxation equation for the nth cycle becomes:

$$\frac{d\theta_r(n)}{d\eta} = -(\theta_r(n) - \theta_r^2(n)) \cdot \tag{24}$$

The time spent in the relaxation zone is evaluated from the circulation time. Based on the assumption that 90% of the liquid volume constitutes the relaxation zone and using the expression for circulation time for Rushton turbines[27] having $D/T = 0{\cdot}5$, they expressed the circulation time as,

$$\eta_r = 2{\cdot}98\frac{Re}{We}\left(\frac{d}{D}\right)^{-1} \cdot \tag{25}$$

Thus, if $\theta_{ri}(n)$ is known, $\theta_{rf}(n)$, the final state reached by the drop at η_r can be obtained by solving eqn (24).

Any cycle begins with the deformation zone and ends with the relaxation zone. For the first cycle:

$$\eta = 0,\ \theta_{di}(1) = 0 \cdot \tag{26}$$

In general, the deformation at the end of $(n-1)$th cycle is the state of entry into the deformation zone for the nth cycle, and the state of exit from this zone then forms the initial condition for the relaxation zone of the same cycle. Thus:

$$\theta_{di}(n) = \theta_{rf}(n-1) \equiv \theta_i(n) \tag{27}$$

and

$$\theta_{ri}(n) = \theta_{df}(n) \equiv \theta_f(n) \cdot \tag{28}$$

Thus, if the initial condition at the time of entry into the deformation zone for the first cycle is defined, the entire history of the drop can be traced.

The solution of the differential equations for both the zones are:

Deformation zone:

$$\frac{2}{b}\left(\tan^{-1}\left(\frac{\theta_f(n) - (1/2)}{(b/2)}\right) - \tan^{-1}\left(\frac{\theta_i(n) - (1/2)}{(b/2)}\right)\right) = \eta_d;\ n \geq 1; \tag{29}$$

$$\theta_i(1) = \theta_0; \tag{30}$$

where $$b^2 = \left(\frac{d}{d_m^*}\right)^{5/3} - 1; \tag{31}$$

and $$\frac{d_m^*}{D} = 0{\cdot}125\ We^{-0{\cdot}6}\,. \tag{32}$$

Relaxation zone:

$$\frac{\theta_i(n+1)}{1 - \theta_i(n+1)} = \frac{\theta_f(n)}{1 - \theta_f(n)} \exp(-\eta_r)\,. \tag{33}$$

The way a drop breaks following eqns (29) and (33) has been presented by Kumar *et al*[26] through the use of phase portraits. One of the possible phase portraits is shown in Fig 7. Curve A represents $\theta_f(n)$ values attained at the end of deformation

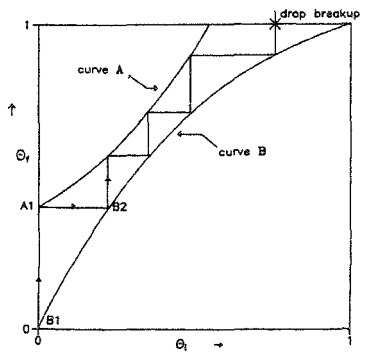

FIG. 7. Phase portrait for multistage drop breakage.

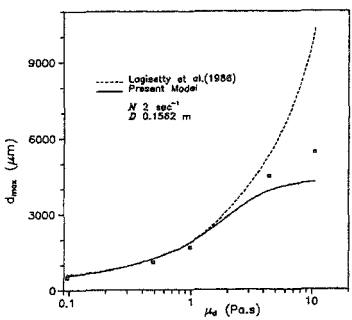

FIG. 8. Effect of μ_d on d_{max}: comparison of the models with experimental data of Wang and Calabrese[14].

period for any $\theta_i(n)$ with which the drop enters the deformation zone. Similarly, curve B represents the residual deformation at the exit of relaxation zone $\theta_i(n)$ when it has entered the zone with a deformation given by $\theta_f(n-1)$. In this figure, curves A and B do not intersect. The history of drop deformation can now be traced in this figure by moving vertically and horizontally until θ_f reaches unity corresponding to breakage. Thus, this figure clearly demonstrates how a drop, which cannot be broken by a single eddy, can be broken by multiple interactions. A situation might arise for a drop, where curves A and B intersect at two points. In such a figure, if an undeformed drop is made the starting point, it will not be broken. For large drops, curves A and B do not intersect and hence they are broken, whereas for very small drops curves A and B invariably intersect at two points which cannot result in breakage. When drop size is slowly decreased, curves A and B, initially non-intersecting, move towards each other until, for a specific drop size, they intersect at just one point. This drop size corresponds to d_{max} as a smaller drop will result in curves A and B intersecting at two points thus not resulting in breakage whereas a slightly larger drop will result in separation of the two curves indicating breakage. The d_{max} therefore is the largest size drop which can have infinite number of recirculations in the vessel without breakage. Mathematically, the concept of two curves intersecting at one point can be expressed as:

$$\theta_i(n) = \theta_i\,(n+1). \tag{34}$$

Further, the slopes of the curves at this point will be the same. Hence,

$$\frac{d\theta_f(n)}{d\theta_i(n)} = \frac{d\theta_f(n)}{d\theta_i(n+1)}\,. \tag{35}$$

Thus d_{max} is that value of the drop diameter for which two steady states (the two intersecting points) of the curves A and B collapse into one.

Kumar *et al*[26] have tested their model with the existing data both with respect to viscosity and interfacial tension. Figure 8 shows the experimental data of Calabrese *et al*[25] on the effect of μ_d on d_{max} along with the predictions made by the model of Kumar *et al*[26] and that of Lagisetty *et al*[10], whose predictions are similar to those made by the correlation of Calabrese *et al*[28]. It is seen that up to a viscosity of 1 Pa.s. predictions made by different models are in reasonable agreement, whereas at higher μ_d values, only the model of Kumar *et al*[26] is able to predict reasonably well. Though the agreement is not excellent, the trends predicted are far different from those of earlier investigators. In fact, this model correctly predicts the decreasing dependence of d_{max} on μ_d from 3/4th power.

Kumar *et al*[26] have also derived the limiting case when μ_d tends to infinity. Their final expression for this limiting case is :

$$\frac{d_{max}}{D} = \left(\frac{2{\cdot}98}{32}\right)^{3/7} \frac{\sigma^{3/7}}{\rho^{3/7}\, N^{6/7}\, D^{9/7}}\,. \tag{36}$$

The above equation shows that even though d_{max} becomes independent of μ_d at very high values of μ_d, it still remains a function of the interfacial tension. The interfacial tension effect at high μ_d values essentially arises out of the relaxation zone, where it influences the relaxation of the drop to the original shape. As this process is driven by the interfacial tension, this variable continues to have reasonably strong effect at high μ_d values also.

Thus, prediction of d_{max} cannot always be analysed through one eddy interaction, but can be the result of not only multiple interactions but also the alternative mechanisms of drop breakage.

5. Breakage frequency and daughter droplet size distribution

For prediction of drop-size distribution in a stirred vessel, under predominantly breakage-dominated conditions, it is necessary to be able to predict breakage frequency and the daughter droplet size distribution. There have appeared two models for breakage frequency, $\Gamma(v)$, but none for the daughter droplet distribution, $\beta(v, v')$. Further, these models can be applied to only inviscid dispersed phases and cannot be used for viscous or rheologically complex dispersed phases. As all the models assume equal breakage of drops, the drop size distribution predicted by them naturally is concentrated near the d_{max}. Experimental measurements, however, show large number of much smaller drops existing in the stirred vessel.

Nambiar *et al*[29] have recently proposed a model where the breakage of a drop into unequal parts is examined. The basic mechanism assumed by them is shown in Fig. 9. Normally, it has been the practice to consider inertial stress to be applied across the

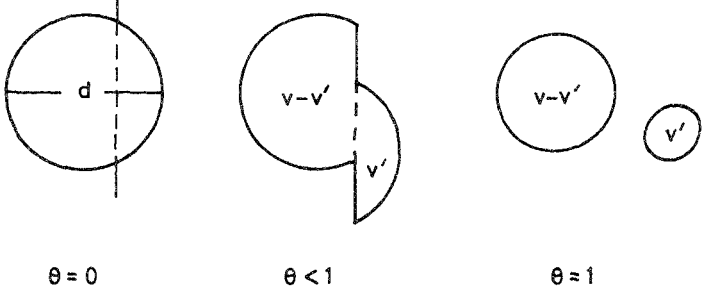

FIG. 9. Unequal breakage of a drop by eddies smaller than its diameter.

diameter of the drop, as the eddy of this size has the highest energy and the longest life time. These authors considered the application of smaller eddies of length scale, l, across the chords of equal length but smaller than the diameter of the drop and found that drops much larger than d_{max} can indeed break by this mechanism. They modified the equations of Lagisetty *et al*[10] to adjust for the interfacial tension stress across the chord so that it reduced to the existing model when the chord became equal to the diameter of the drop. Their governing equation for unequal breakage is:

$$\frac{d\theta}{d\eta} = \frac{C(l/d)^{2/3}}{G} We \left(\frac{d}{D}\right)^{5/3} - (\theta - \theta^2) \tag{37}$$

where the turbulent stress is given by $C\rho_c N^2 D^{4/3} l^{2/3}$ and the nondimensional time η gets modified to:

$$\eta = \frac{\sigma G}{d\mu_d} t\,; \tag{38}$$

$$G = \frac{\left(\frac{\nu - \nu'}{\nu}\right)^{2/3} + \left(\frac{\nu'}{\nu}\right)^{2/3}}{2^{1/3}}\,. \tag{39}$$

On breakage, the new droplet formed is given by

$$\frac{\nu'}{\nu} = \frac{1}{2}\left[1 \mp \frac{3}{2}\sqrt{1 - x^2} \pm \frac{1}{2}(1 - x^2)^{3/2}\right] \tag{40}$$

where

$$x = l/d. \tag{41}$$

Equation (37) is solved with the initial condition

$$\theta = 0 \text{ at } \eta = 0\,. \tag{42}$$

The dimensionless breakage time to reach $\theta = 1$, obtained by solving eqn (37), is:

$$\eta_B = \eta(\theta = 1) = \frac{2}{\sqrt{\alpha}} \tan^{-1} \frac{1}{2\sqrt{\alpha}} \tag{43}$$

where

$$\alpha = \frac{C(l/d)^{2/3}}{G} We \left(\frac{d}{D}\right)^{5/3} - \frac{1}{4}\,. \tag{44}$$

As the drop has to break within the life time, $\frac{\sigma G}{d\mu_d}\bar{T}$, of the eddy, it puts a constraint of finding $l \leq d$, that satisfies the following:

$$\frac{2}{\sqrt{\alpha}} \tan^{-1} \frac{1}{2\sqrt{\alpha}} \leq \left(\frac{Re\ G}{We}\right)\left(\frac{d}{D}\right)^{-1/3}\left(\frac{l}{d}\right)^{2/3}. \tag{45}$$

Their calculations show that extremely small values of l do not satisfy the above constraint. However, for drops larger than d_{max} there is a range of eddy sizes, for which the constraint is satisfied. The drop can be broken from a smaller eddy, l_{min}, to the eddy of the size of the drop itself. The range of eddy sizes capable of drop breakage diminishes rapidly as the drop size comes closer to d_{max} and reaches to a limit of a single value at d_{max}. Thus, drops of size d_{max} only can undergo equal breakage, but they do not break. All drops larger than d_{max} will invariably break into unequal parts. This finding is in complete contrast to the earlier assumption of equal breakage, which is, however, reasonable for predicting d_{max} as this model shows that near d_{max}, the drops do tend to break into equal parts. Combining the unequal breakage concept with the eddy-sized distribution existing in the vessel, these authors have proposed a new model which simultaneously predicts both the breakage frequency and the distribution of the daughter droplets. Breakage frequency is viewed as the number of times a droplet of given size will break in a unit time, when placed in the stirred vessel. This naturally must depend on the frequency with which it interacts with eddies of the right size. Thus, before it loses its identity through breakage it may interact with a number of eddies of different sizes. Nambiar *et al*[29] assumed the interactions to occur sequentially. A typical sequence of interactions is shown in Fig. 10. In this figure, the drop first interacts with an eddy of size below $l_{min}(d)$ during its life time but does not break. It is then interacted on by a much larger eddy which merely convects it. It repeats the cycle once more before it interacts with an eddy in size range (l_{min} (d), d). This eddy breaks the drop as it falls in the right size. This model of interaction is employed to obtain an expression for the expected survival time of the drop.

Expected survival time = Expected number of ineffective eddies × Expected life time of an ineffective eddy + Expected breakage time with the final eddy

$$t_s = \frac{q}{p}\int_{L_K}^{D} \bar{T}(l) f(l|l \notin (l_{min},\ d))\ dl + \int_{L_K}^{D} t_b(l,\ d)\ f\ (l|l \in (l_{min},\ d))dl \tag{46}$$

where

$$p = \int_{l_{min}}^{d} f(l)\ dl\ . \tag{47}$$

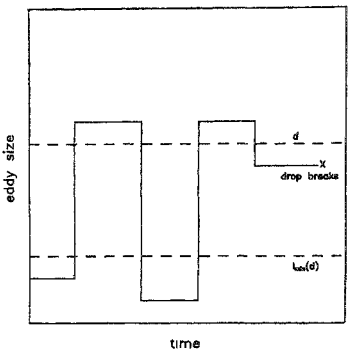

FIG. 10. Drop interaction pattern with turbulent eddies in the vessel.

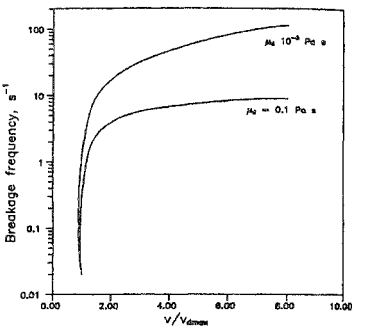

FIG. 11 Breakage frequency variation with drop size.

It is necessary to obtain an expression for $f(l)$ to be able to use eqn (46). At fully developed turbulence, the stirred vessel is populated with eddies from size D down to the Kolmogorov-scale eddies L_K. In these lowest-scale eddies, energy dissipation occurs, whereas in the large-scale eddies, dissipation is negligible. The value of L_K can be obtained by

$$L_K = \left(\frac{\nu^3}{\epsilon}\right)^{1/4} \cdot \tag{48}$$

The eddies of size range (L_K, D) derive the energy from mean flow at the upper end of the eddy size which is then cascaded down to smaller and smaller eddies without any significant attenuation. If l^3 is taken as the measure of the volume of the eddy, then the eddy-size distribution has the form:

$$f(l) = \frac{C_f}{l^3} \cdot \tag{49}$$

The normalisation constant C_f is obtained by using the basic requirement of $f(l)$, *i.e.*,

$$\int_{L_K}^{D} f(l)\, dl = 1 \cdot \tag{50}$$

The C_f then works out to be:

$$C_f = 2\,\frac{(DL_K)^2}{(D^2 - L_K^2)}\,. \tag{51}$$

The breakage frequency is directly obtained as the reciprocal of the expected time of survival. Thus,

$$\Gamma(v) = \frac{1}{t_s(v)}\,. \tag{52}$$

A set of typical curves of breakage frequency are shown in Fig. 11, where breakage frequency calculated through eqn (52) is plotted *versus* drop volume non-dimensionalised with $v_{d\,max}$. It is seen that at d_{max}, the breakage frequency is zero, but rises sharply thereafter. This picture is thus consistent with the notion that drops of size d_{max} will not break. Further, calculations for two viscosities show that the breakage frequency falls as the dispersed-phase viscosity is raised. Similarly, lowering of frequency was also found with increase in interfacial tension. These trends are qualitatively expected as increase in μ_d or σ makes the breakage process more difficult.

The daughter droplet distribution is obtained directly from the eddy-size distribution as the knowledge of the scale of drop-breaking eddy is directly related to the volume v' of the daughter droplet. Thus:

$$\beta(v',v) = \frac{1}{2}\,\frac{f(l|l_{min} \le l \le d)}{\left|\left(dv'/dl\right)\right|}\,. \tag{53}$$

$\left|\dfrac{dv'}{dl}\right|$ can be evaluated using the geometric relationship between l and v'. Profiles of $\beta(v, v')$ computed for different values are presented in Fig. 12. It is seen that the distribution is symmetric about $v'/2$, as expected from binary breakage. It is also seen that asymmetric breakage is preferred.

As the breakage frequency and daughter droplet distributions cannot be directly measured, the models for them are tested by solving the population balance equations and comparing the predicted drop size distributions with the ones obtained experimentally. Such a comparison is shown in Fig. 13, where the calculated distributions are compared with the experimental results of Calabrese *et al*[25]. It is seen that the new model is able to explain these results well.

6. Conclusions

Though the drop breakage in stirred vessel is a three-dimensional problem, it can be successfully reduced to a single-dimensional framework through the use of a Voigt element. This framework captures the basic features of the breakage phenomenon, and can be used for predictive purposes for obtaining d_{max} values for not only a variety of dispersed-phase rheologics but also when surfactants or drag-reducing agents are present in the continuous phase.

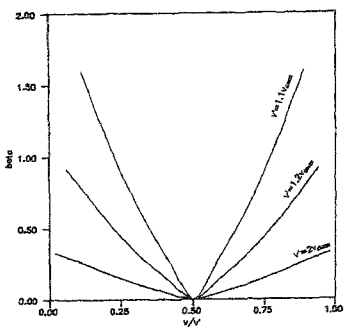

FIG 12. The daughter droplet distribution.

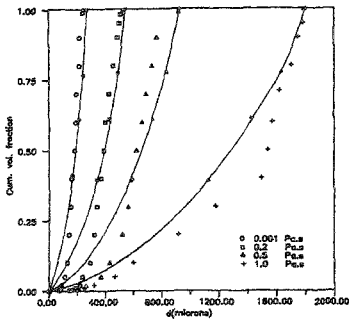

FIG. 13. Drop size distribution: comparison of the model of Nambiar *et al*[2] with the existing data.

The unexpected behaviour of d_{max} with increase in ϕ cannot be explained by turbulent mechanism. Alternative mechanisms involving elongational and shear flows have to be invoked to explain these results. A large number of simplifications regarding the flow have to be made to make the analysis tractable. Hence these models, though able to explain the qualitative trends, can at best be used to make order of magnitude estimates. More work needs to be done in defining the flow field with more rigour and also for obtaining drop breakage conditions under complex flow fields.

The new model of breakage frequency and daughter droplet distribution, based on unequal breakage, though still through a single-dimensional framework, is able to satisfactorily explain quite a few of the experimental results available in literature. However, it may require fine-tuning, particularly regarding breakage near d_{max}.

At present no models are available for breakage frequency based on either alternative or multistage breakage mechanisms. These models need to be developed and verified.

Nomenclature

a	interfacial area per unit volume of the dispersion, m^{-1}
b	defined in the text (eqn 31)
C_1, C_2	constants
C_f	defined in the text (eqn 51)
Ca_e, Ca_s	critical capillary numbers for elongational and shear-flow breakage

d	drop size, m
d_{max}	maximum stable drop diameter through turbulent mechanism, m
$(d_{max})_e$, $(d_{max})_s$	maximum stable drop diameters through elongational and shear mechanisms respectively, m
d_m	defined in the text (eqn 32)
D	diameter of the impeller, m
$f_o(v)$	escape rate of drops, s^{-1}
G	strain rate, s^{-1}
G_e	strain rate for elongational flow, s^{-1}
G_s	shear rate, s^{-1}
K	constant in power law model, N m^{-2} s^n
l	length scale of the eddy, m
$l_{min}(d)$	size of smallest eddy capable of breaking a drop of diameter d, m
L	blade length, m
L_K	Kolomogorov length scale, m
n	power law index
N	revolutions per second of the stirrer, s^{-1}
$n(v, t)dv$	number of droplets in the size range $(v, v + dv)$ at time t in a unit volume of dispersion, m^{-3}
$N_o(v)dv$	number feed rate of drops in the size range $(v, v + dv)$ per unit volume of the dispersion, m^{-3} s^{-1}
N_{Re}	tank Reynolds number, $\rho_c D^2 N/\mu_c$
p	probability of the eddy interacting with the drop being of a size that can cause breakage of the drop
$q(v, v')$	frequency of coalescence between drops of size v and v', m^3 s^{-1}
Re	Reynolds number, $D^n (ND)^{2-n} \rho_c/[K\, 2^{n-3} (3 + 1/n)^n]$
t	time, s
t_b	characteristic breakage time, s
t_c	circulation time, s
t_s	expected survival time, s
$\bar{T}$	mean life time of the eddy, s
$\overline{u^2(d)}$	mean square velocity fluctuation across length scale d, m^2 s^{-2}
$\overline{u_\phi^2(d)}$	mean square velocity fluctuation across d for liquid hold up ϕ, m^2 s^{-2}
We	Weber number, $\rho_c N^2 D^3/\sigma$
x	defined in the text (eqn 41)

Greek letters

α	dimensionless quantity defined in the text (eqn 44)
ϕ	dispersed phase hold-up
$\beta(v, v')dv$	fraction of daughter droplets in size range $(v, v + dv)$ when a drop of size v' breaks
ϵ	power dissipation per unit mass, m^2s^{-3}
$\Gamma(v)$	breakage frequency, s^{-1}
$\gamma(v)$	number of daughter droplets formed per breakage
ρ_c, ρ_e	continuous phase and emulsion density, respectively, kg m^{-3}
τ_t	mean turbulent stress, N m^{-2}
τ_o	yield stress, N m^{-2}
σ	interfacial tension, N m^{-1}
η	dimensionless time
η_d	dimensionless eddy life time
η_r	dimensionless residence time in relaxation zone
μ_c	continuous phase viscosity, Pa.s
μ_d	dispersed phase viscosity, Pa.s
μ_e	emulsion viscosity, Pa.s
θ	dimensionless drop deformation
θ_o	initial deformation at the beginning of the first cycle (normally zero)
$\theta_d(n)$	deformation in nth cycle in the deformation zone
$\theta_r(n)$	deformation in nth cycle in the relaxation zone
$\theta_i(n)$	deformation at the beginning of deformation cycle for the nth cycle
θ_f the (n)	deformation at the end of deformation zone for the nth cycle

References

1. BOURNE, J. R., KOZICKI, F. AND RYS, P. — Mixing and fast chemical reactions I — Test reactions to determine segregation, *Chem. Engng Sci.*, 1981, **36**, 1643–1648.
2. BELEVI, H., BOURNE, J R. AND RYS, P. — Mixing and fast chemical reactions II. Diffusion-reaction model for CSTR, *Chem. Engng Sci.*, 1981, **36**, 1649–1654.
3. BOURNE, J. R., KOZICKI, F., MOERGELI, U. AND RYS, P. — Mixing and fast chemical reactions III. Model–experiment comparisons, *Chem. Engng Sci.*, 1981, **36**, 1655–1663.
4. ANGST, W., BOURNE, J. R AND SHARMA, R. N. — Mixing and fast chemical reactions IV. The dimensions of the reaction zone, *Chem. Engng Sci.*, 1982, **37**, 585–590.
5. SCHUMPE, A. AND DECKWER, D. W. — Analysis of chemical methods for determination of interfacial areas in gas-in-liquid dispersions with non-uniform bubble sizes, *Chem. Engng Sci* , 1982, **35**, 2221–2233.
6. HULBURT, H. M. AND KATZ, S. L. — Some problems in particulate technology, *Chem. Engng Sci.*, 1964, **19**, 555–574.

7. KOLMOGOROV, A. N — On the atomisation of droplets in a turbulent flow, *Doklady Akad. Nauk*, USSR, 1949, **66**, 825–828.

8. HINZE, J. O — Fundamentals of the hydrodynamic mechanism of splitting in dispersion processes, *AIChE J.*, 1955, **1**, 289–295

9. SPROW, F. B — Distribution of drop sizes produced in turbulent liquid–liquid dispersion, *Chem. Engng Sci.*, 1967, **22**, 435–442.

10. LAGISETTY, J. S., DAS, P. K., KUMAR, R AND GANDHI, K. S. — Breakage of viscous and non-Newtonian drops in turbulent dispersions, *Chem. Engng Sci.*, 1986, **41**, 65–72

11. COULALOGLOU, C. A AND TAVLARIDES, L. L. — Drop size distributions and coalescence frequencies of liquid–liquid dispersions in flow vessels, *AIChE J.*, 1976, **22**, 289–297

12. ARAI, K., KONNO, M., MATUNAGA, Y. AND SAITO, S. — Effect of dispersed phase viscosity on the maximum stable drop size for break-up in turbulent flow, *J. Chem. Engng Jap.*, 1977, **10**, 325–330.

13. KONNO, M., ARAI, K. AND SAITO, S. — The effect of stabilizer on coalescence of drops in suspension polymerization of styrene, *J. Chem Engng Jap* 1982, **15**, 131–135.

14. WANG, C. Y AND CALABRESE, R V. — Drop breakup in turbulent stirred-tank contactors; Part II: Relative influence of viscosity and interfacial tension, *AIChE J.*, 1986, **32**, 667–676.

15. DAVIES, J. T. — Drop sizes of emulsions related to turbulent energy dissipation rates, *Chem. Engng Sci.*, 1985, **40**, 839–842.

16. RALLISON, J. M. — The deformation of small viscous drops and bubbles in shear flow, *A. Rev. Fluid Mech*, 1984, **16**, 45–66

17 KOSHY, A., DAS, T. R., KUMAR, R. AND GANDHI, K. S. — Breakage of viscoelastic drops in turbulent-stirred dispersions, *Chem. Engng Sci.*, 1988, **43**, 2625–2631.

18. KOSHY, A., DAS, T. R. AND KUMAR, R. — Effect of surfactants on drop breakage in turbulent stirred dispersions, *Chem. Engng Sci.*, 1988, **43**, 649–654.

19. KOSHY, A., KUMAR, R AND GANDHI, K. S. — Effect of drag-reducing agents on drop breakage in stirred dispersions, *Chem. Engng Sci.*, 1989, **44**, 2113–2120.

20. GANDHI, K. S. AND KUMAR, R. — An elongational flow model for drop breakage in stirred turbulent dispersions, *Chem. Engng Sci.*, 1990, **45**, 2998–3001

21. LATS, M. K. AND FRISHMAN, F. A. — Development of the techniques and investigation of turbulent energy at the axis of two-phase turbulent jet, *Fluid Mech*, 1974, **8**, 304–307 (translation from Russian).

22. KUMAR, S, KUMAR, R AND GANDHI, K. S — Alternate mechanisms of drop breakage in stirred vessels, *Chem Engng Sci*, 1991, **46**, 2483–2489

23. GROSSO, J. L., BRICENO, M. I., PATERNO, J. AND LAYRISSE, I. — Influence of crude oil and surfactant concentration on the rheology and flowing properties of heavy crude oil-in-water emulsions, *Surfactants in solutions* (ed., K. L. Mittal), 1986, pp 1653–1673, Plenum.

24. TAYLOR, G. I. — The formation of emulsions in definable fields of flow, *Proc. R. Soc. A*, 1934, **146**, 501–523.

25. CALABRESE, R. V., CHANG, T. P. K. AND DANG, P. T. — Drop breakup in turbulent stirred-tank contactors, part I: Effect of dispersed phase viscosity. *AIChE J.*, 1986, **32**, 657–666.

26. KUMAR, S., KUMAR, R. AND GANDHI, K. S. — A multi-stage model for drop breakage in stirred vessels, *Chem. Engng Sci.*, 1992, **47**, 971–980

27. HOLMES, D. B., VONCKEN, R. M. AND DEKKER., J. A — Fluid flow in turbine-stirred, baffled tanks–I, Circulation time, *Chem. Engng Sci.*, 1964, **19**, 201–208.

28. CALABRESE, R. V., WANG, C. Y. AND BRYNER, N. P. — Drop breakup in turbulent stirred-tank contactors II, Correlation for mean size and drop size distribution, *AIChE J.*, 1986, **32**, 677–681.

29. NAMBIAR, D. K. R., KUMAR, R., DAS, T. R AND GANDHI, K. S. — A new model for the breakage frequency of drops in stirred turbulent dispersions, *Chem. Engng Sci.* (in press).